Electronic Supplementary Material (ESI) for Physical Chemistry Chemical Physics.

Supporting Information

Partially Delocalized Charge in Crystalline Co-S-Se/NiO_x Nanocomposites for Boosting Electrocatalytic Oxygen Evolution

Wei Deng[1], Yuping Gai[1], Haitao Duan[1], Zhide Chen[1], Xiaojun Hu[1], Sheng Han[1], Niwei Xu[2], Boying Zhang[3], Shanlin Qiao[3], Zijian Yao[1], Jun Yu[1], Fei Jiang[1*]*

[1] College of Chemical and Environmental Engineering, Shanghai Institute of Technology, Haiquan Road 100, Shanghai 201418, China.

[2] College of Medicine Engineering, Hunan Traditional Chinese Medical College, Xueshi Road 300, Hunan 410208, China.

[3] College of Chemistry and Pharmaceutical Engineering, Hebei University of Science and Technology, Yuxiang Street 26, Shijiazhuang 050018, China.

The DFT calculation:

All calculations were carried out using the CASTEP program package implanted in Materials Studio of Accelrys Inc.[1] The exchange–correlation functional under the generalized gradient approximation (GGA) with norm-conserving pseudopotentials and Perdew–Burke–Ernzerhof (PBE) functional was adopted to describe the electron–electron interaction.[2] An energy cutoff of 400 eV was used. The ternary Co-S-Se alloy monolayer and its corresponding binary CoS_2 and $CoSe_2$ monolayer slab model was employed to simulate the surface properties. The reasonable vacuum layers were set around 15 Å in the z-direction for avoiding interaction between planes. A 4×4×1 Monkhorst Pack k-point sampling was chosen for the well converged energy values. Geometry optimizations were pursued until the force on each atom falls below the convergence criterion of 0.02 eV/Å and energies were converged within 10^{-5} eV.

The Volmer reaction (Equation S1): $H_2O + M + e^- \rightarrow M\text{-}H^* + OH^-$, (1)

In the alkaline environment, the overall OER process at the anode can be described by the following four-step associative mechanism (Equation S2-S5):

$OH^- + * \rightarrow OH^* + e^-$, (2)

$OH^* + OH^- \rightarrow O^* + H_2O + e^-$, (3)

$O^* + OH^- \rightarrow OOH^* + e^-$, (4)

$OOH^* + OH^- \rightarrow O_2 + H_2O + e^-$, (5)

Where * and M* represent the active site and the adsorbed intermediate on the surface, respectively.

The Gibbs free energy change for steps 2–5 can be expressed as follows:

$\Delta G_1 = \Delta G_{OH*} - eU$, (6)

$\Delta G_2 = \Delta G_{O*} - \Delta G_{OH*} - eU$, (7)

$\Delta G_3 = \Delta G_{OOH*} - \Delta G_{O*} - eU$, (8)

$\Delta G_4 = 4.92[eV] - \Delta G_{OOH*} - eU$, (9)

Where U is the applied voltage, in this study, U=0, and the total free energy (ΔG) to form one molecule of O_2 was fixed at the value of 4.92 eV in order to avoid the calculation of the O_2 bond energy, which is difficult to determine accurately within GGA-DFT.

The Gibbs free energy changes of intermediates adsorbed on the surface of catalysts were calculated with zero-point energy and entropy corrections using the following computational formula: $\Delta G_{ads} = \Delta E_{ads} + \Delta ZPE - T\Delta S$, (10)

Where ΔZPE, T and ΔS are the contributions to the free energy from the zero-point vibration energy, temperature and entropy, respectively. The zero-point energies are calculated from the vibration frequencies. The values of ΔZPE were determined by the computed vibrational frequencies and the –eU term represents the external by U imposed on each step. The entropies are taken from standard tables for molecules. Gas phase H_2O at 0.035 bar is used as the reference state because at this pressure gas phase H_2O is in equilibrium with liquid water at 298 K. The theoretical reaction overpotential η can be obtained evaluating the difference between the minimum voltage needed for the OER and the corresponding voltage needed for changing all the free-energy steps into downhill.

The adsorbed intermediate free energy change ΔE_{ads} for steps 2–5 can be expressed as follows:

$\Delta E_{OH*} = E(OH*) - E(*) - [E(H_2O - 1/2\ E(H_2))]$, (11)

$\Delta E_{O*} = E(O*) - E(*) - [E(H_2O) - E(H_2)]$, (12)

$\Delta E_{OOH*} = E(OOH*) - E(*) - [2E(H_2O) - 3/2\ E(H_2)]$. (13)

Where E(*), E(OH*), E(O*) and E(OOH*) are the total energy of the clean surface and the adsorbed surface with three intermediates, respectively. $E(H_2O)$, $E(H_2)$ and $E(O_2)$ are the computed energies for the sole H_2O, H_2 and O_2 molecules, respectively.

The theoretical overpotential η can then be defined as Equation S14:

$\eta = \max[\Delta G_1, \Delta G_2, \Delta G_3, \Delta G_4]/e - 1.23$ [V]. (14)

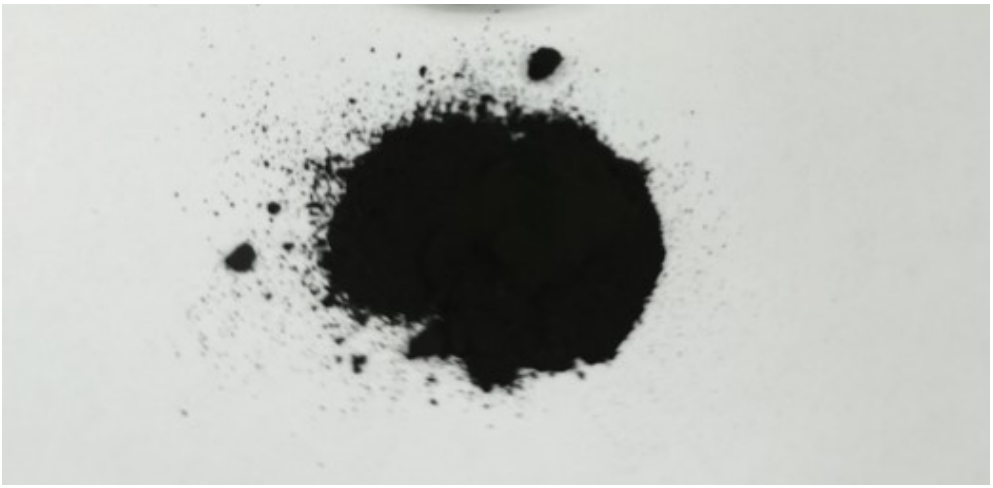

Figure S1. The photograph of $Co_{0.45}S_{0.38}Se_{0.17}$ nanosheets.

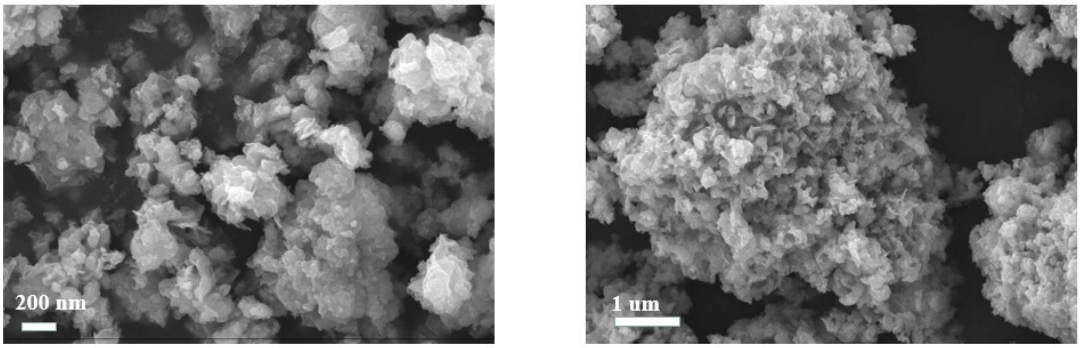

Figure S2. SEM of $Co_{0.45}S_{0.38}Se_{0.17}$ nanosheets.

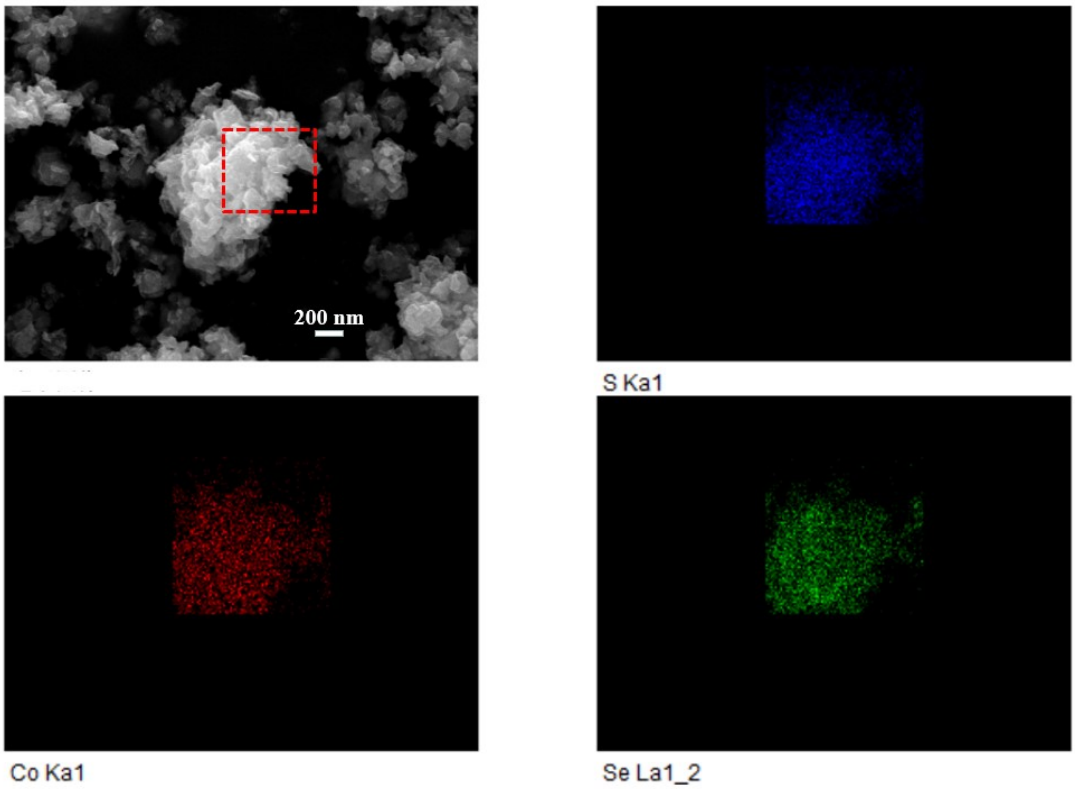

Figure S3. The SEM energy dispersive X-ray spectroscopy (EDS) elemental mapping images of $Co_{0.45}S_{0.38}Se_{0.17}$ nanosheets.

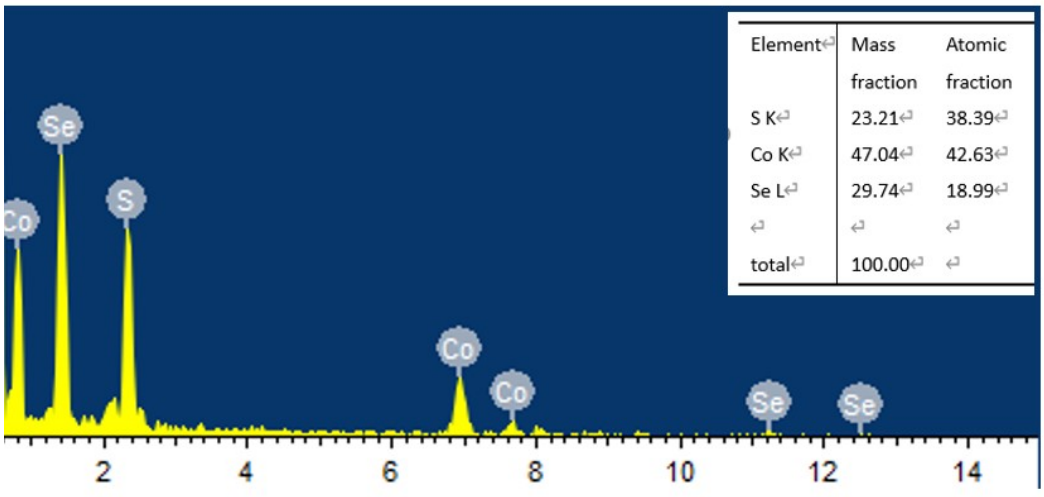

Figure S4. The EDS spectrum of Co, S and Se elements in the $Co_{0.45}S_{0.38}Se_{0.17}$ nanosheets.

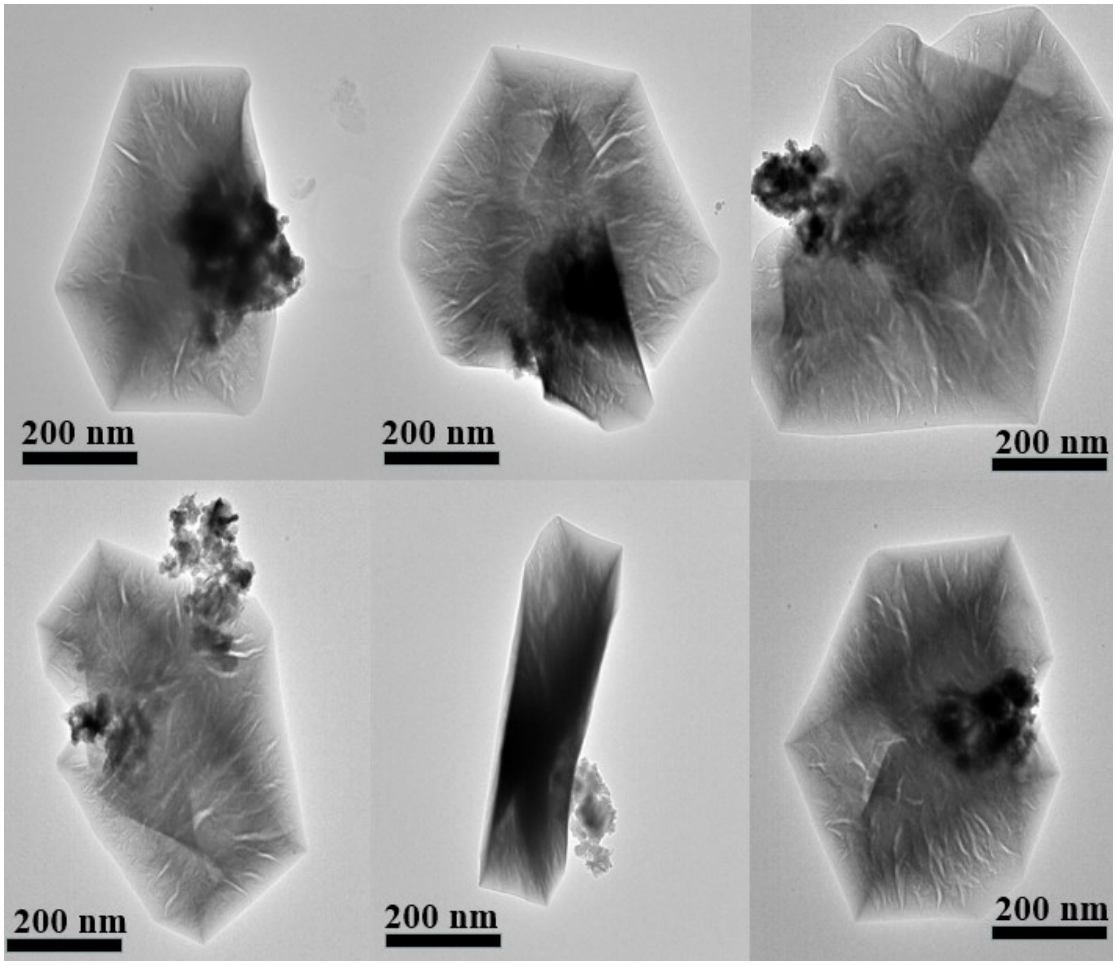

Figure S5. The HRTEM spectrum of the $Co_{0.45}S_{0.38}Se_{0.17}$ nanosheets.

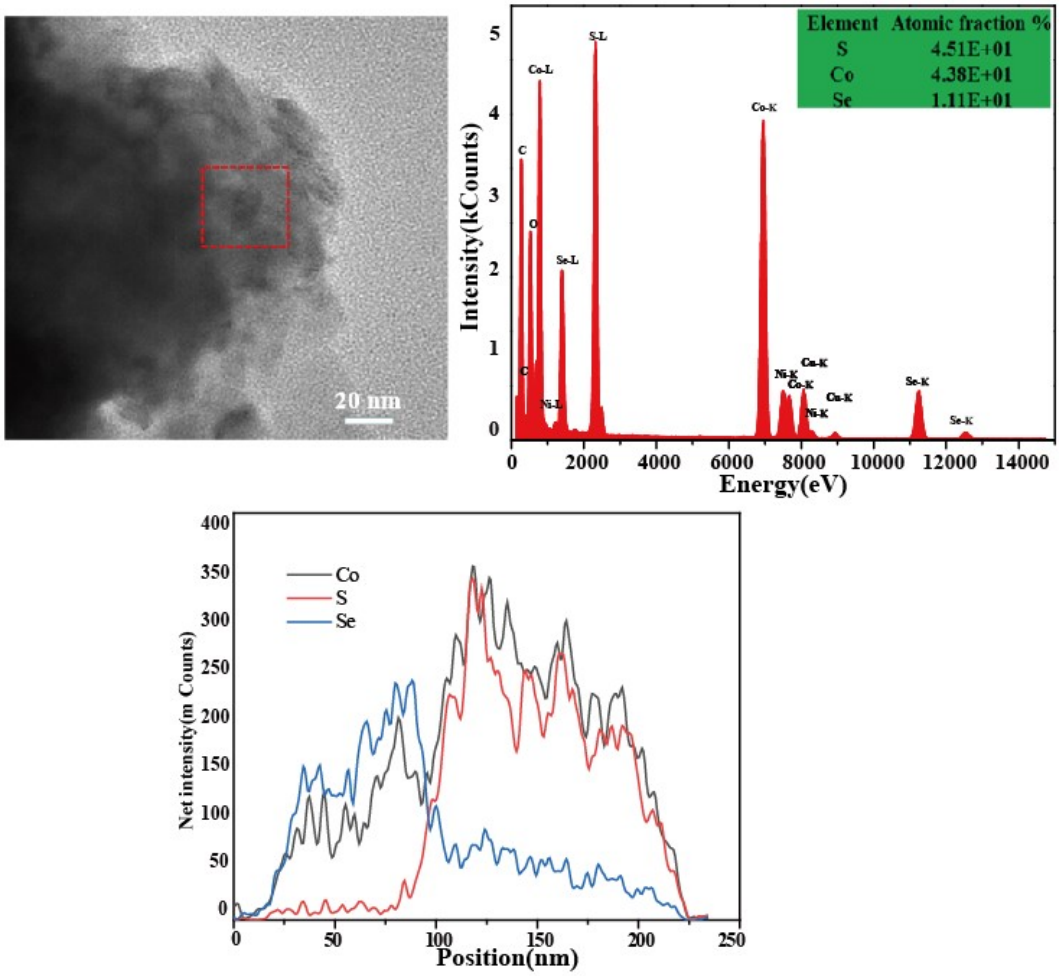

Figure S6. HRTEM images and element distribution of the $Co_{0.45}S_{0.38}Se_{0.17}$ nanosheets.

X-ray photoelectron spectroscopy (XPS)

XPS full analysis results are shown in **Figure S7-S8**, and the valence band maximum (VBM) is shown in **Figure S9**. All the spectra are adjusted according to the standard value of C 1s peak at (284.6 ± 0.1) eV.[3] Decomposition of the XPS spectrum reveals Co, S and Se characteristic peaks.

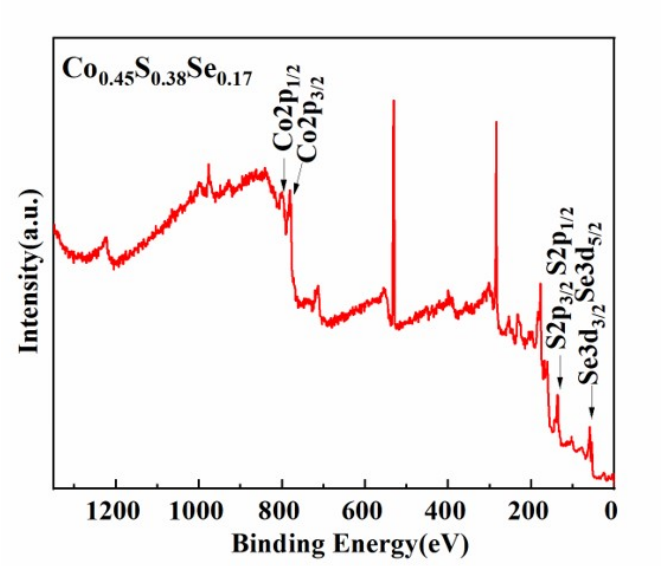

Figure S7. Full scans of XPS spectra for $Co_{0.45}S_{0.38}Se_{0.17}$ nanosheets.

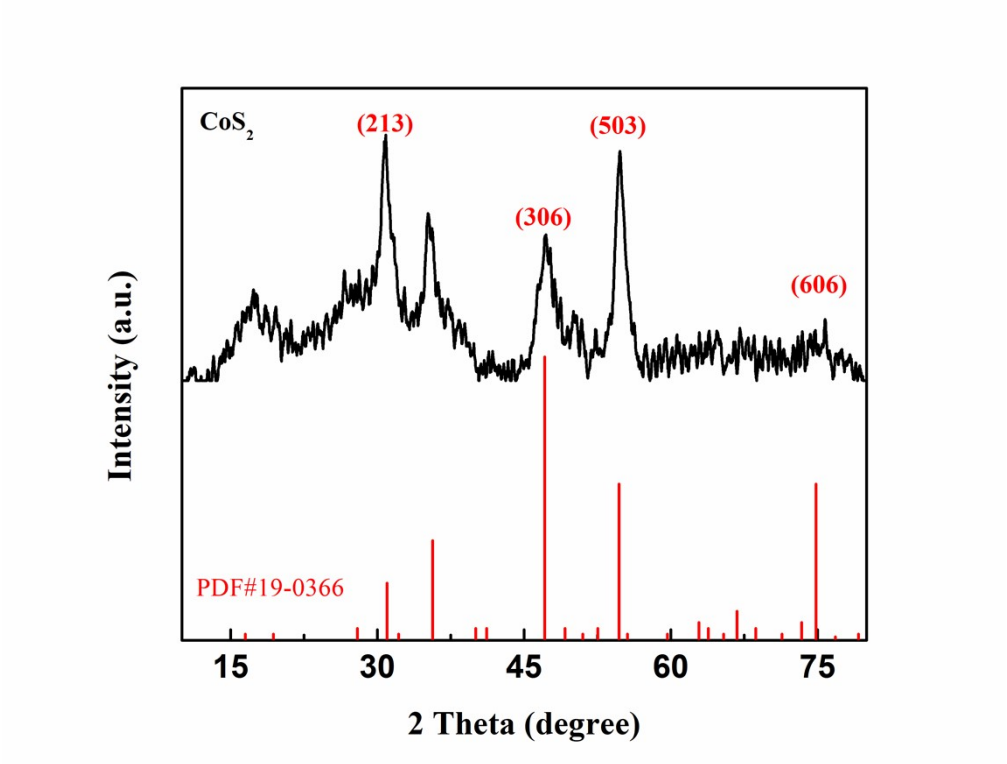

Figure S8. (A) XRD for CoS_2.

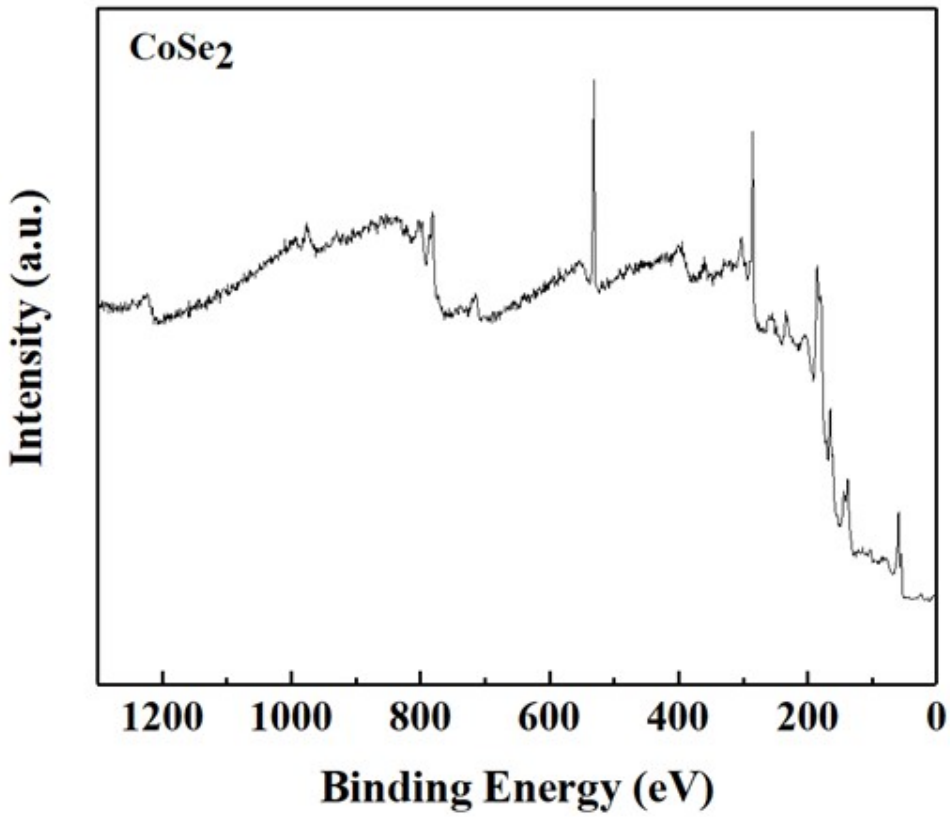

Figure S8. (B) Full scans of XPS spectra for $CoSe_2$.

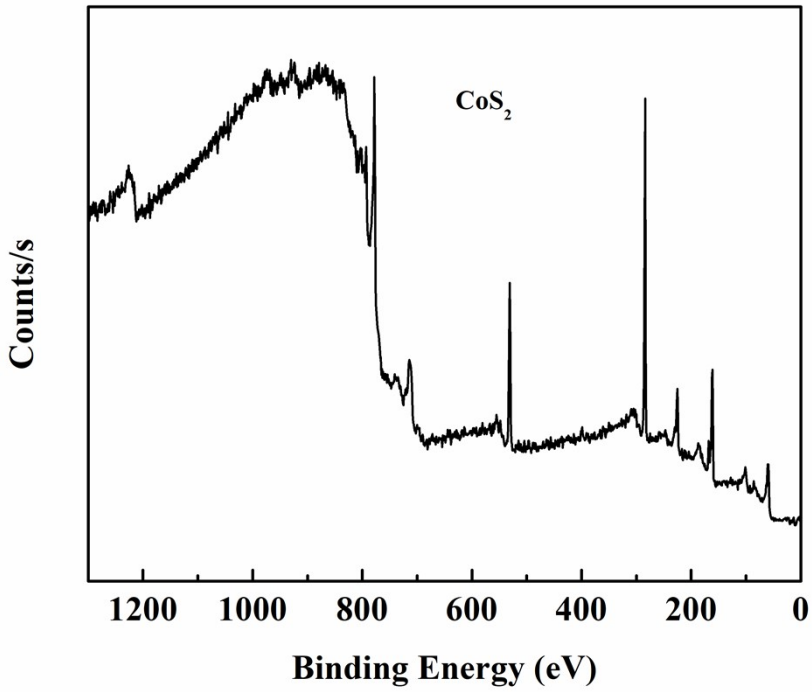

Figure S8. (C) Full scans of XPS spectra for CoS_2.

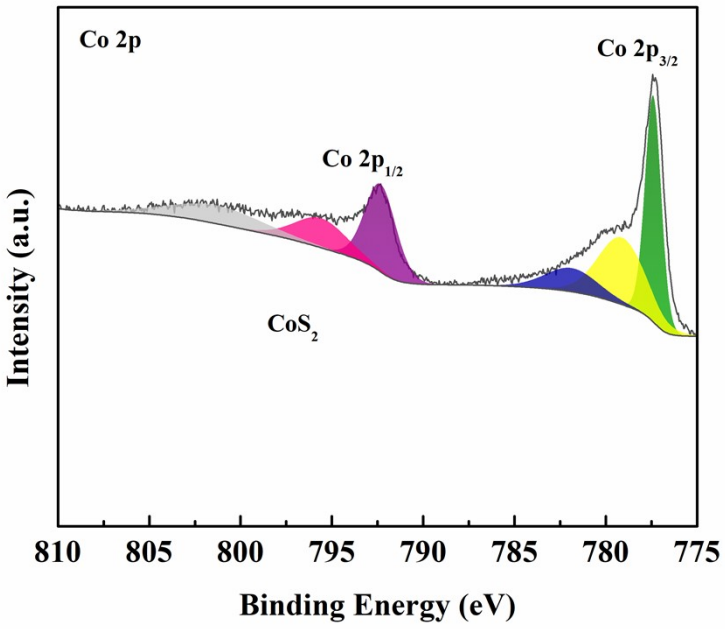

Figure S8. (D) Co 2p spectra for CoS_2.

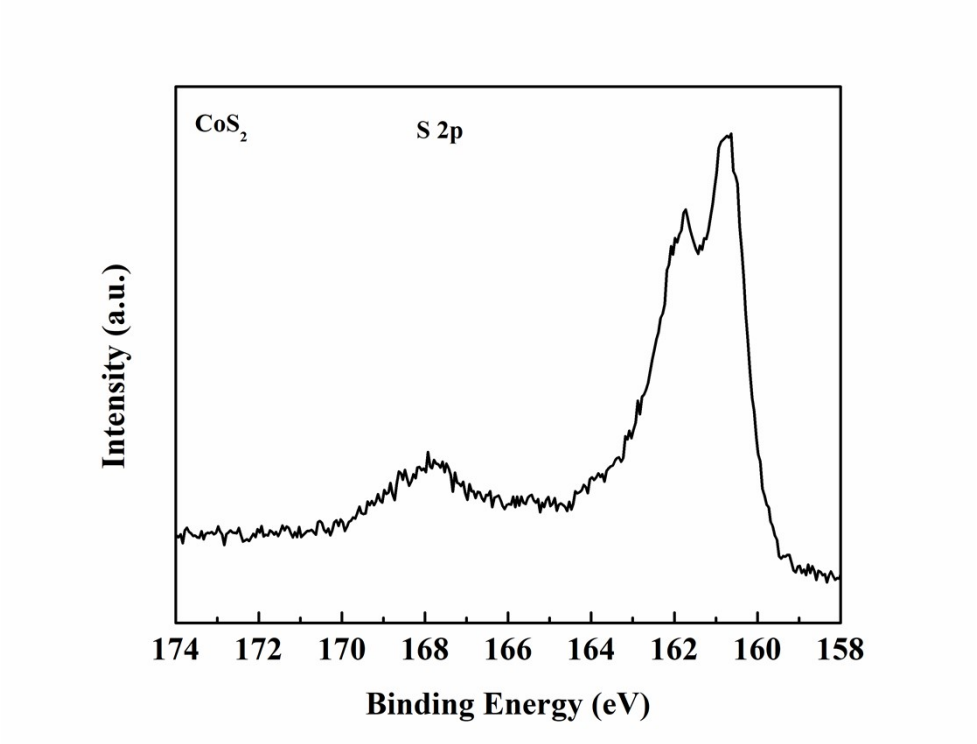

Figure S8. (E) S 2p spectra for CoS_2.

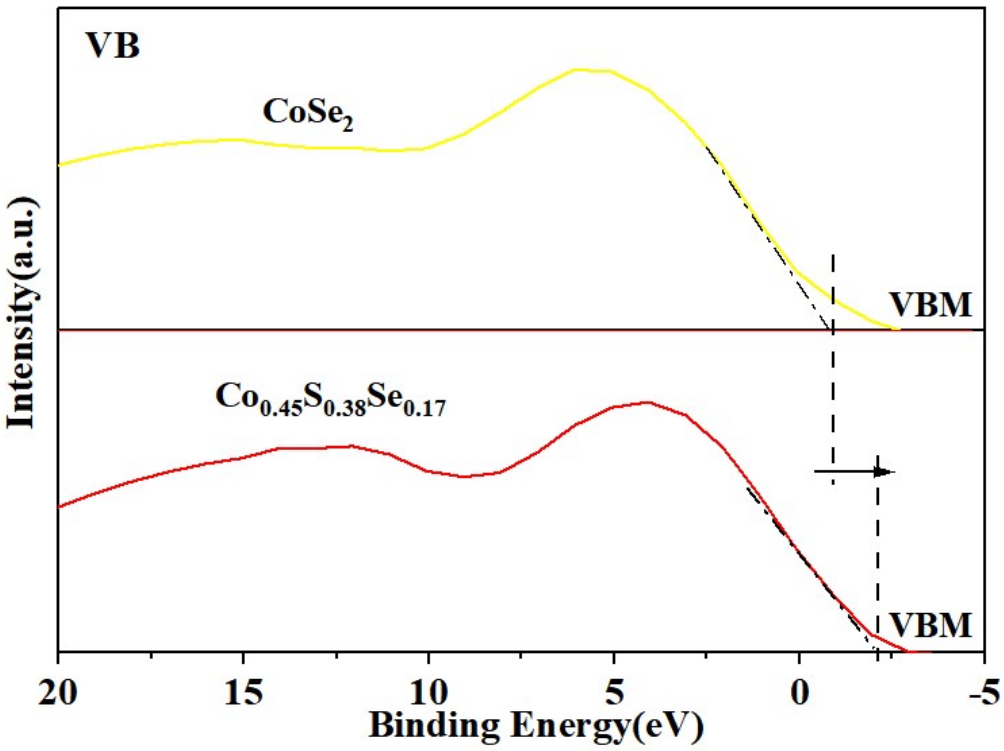

Figure S9. Valence band XPS spectra of $Co_{0.45}S_{0.38}Se_{0.17}$ and $CoSe_2$.

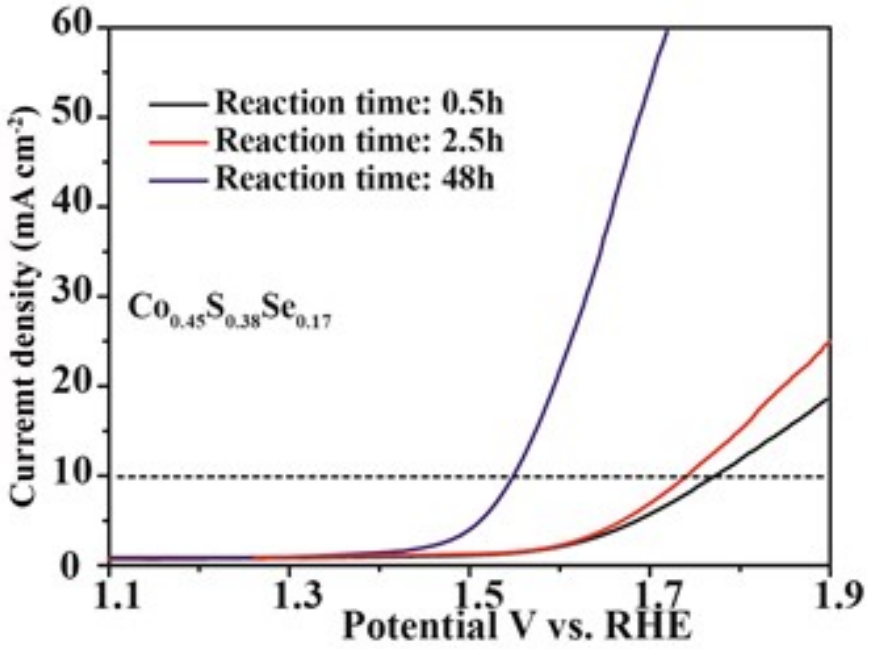

Figure S10. LSV curves of $Co_{0.45}S_{0.38}Se_{0.17}$ products obtained at 200 °C for 0.5 h (black line), 2.5 h (red line) and 48 h (blue line).

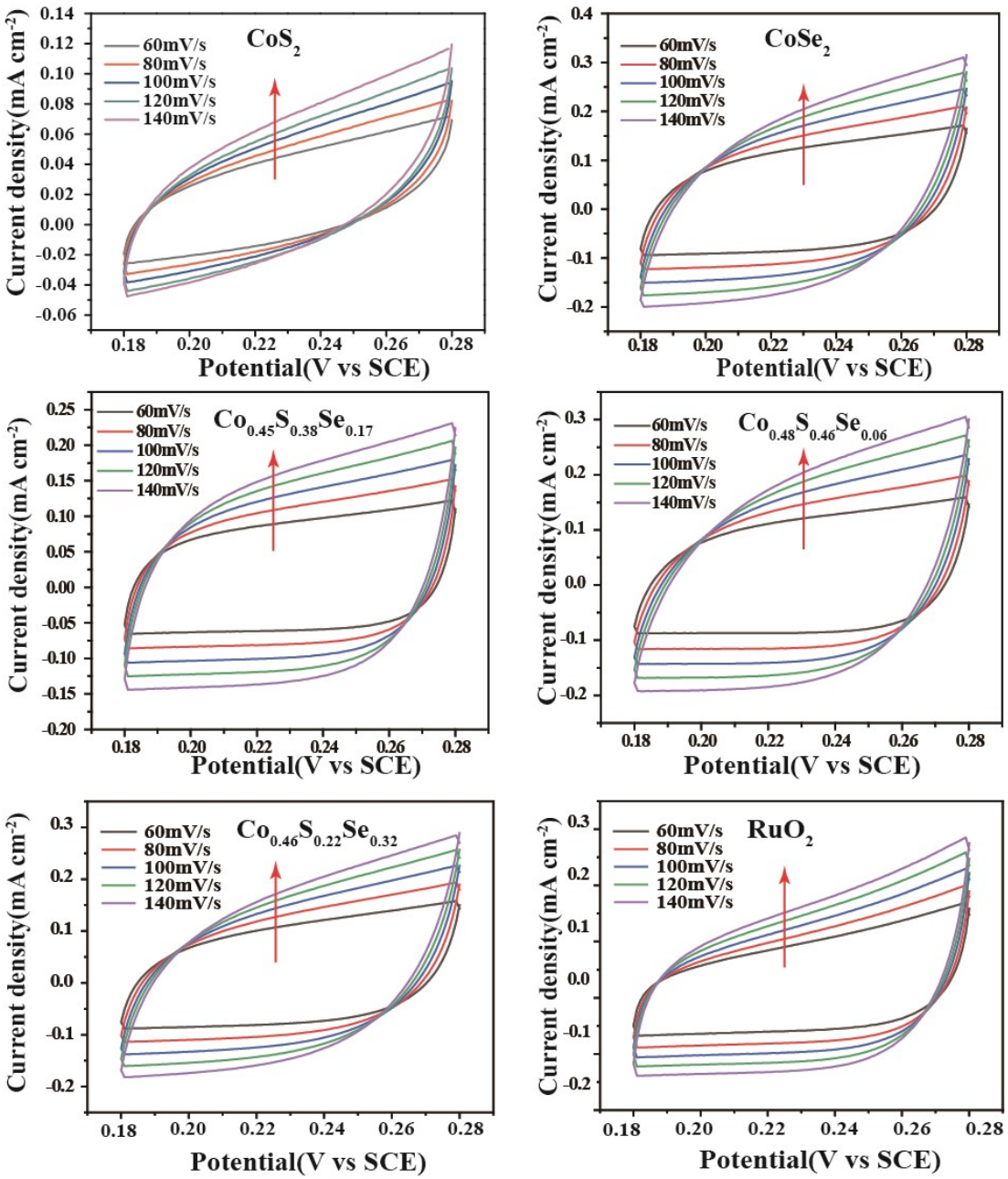

Figure S11. CV curves of CoS_2, $Co_{0.48}S_{0.46}Se_{0.06}$, $Co_{0.45}S_{0.38}Se_{0.17}$, $Co_{0.46}S_{0.22}Se_{0.32}$, $CoSe_2$ and RuO_2 in the double layer region at different scan rates.

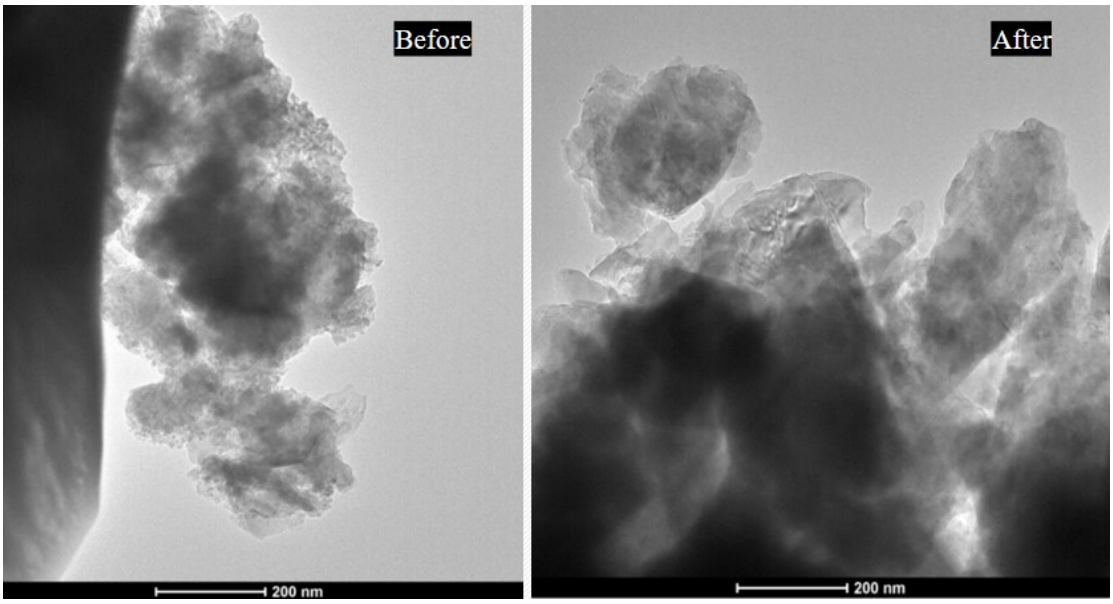

Figure S12. The TEM images showed that the Co-S-Se before and after the stability test for OER.

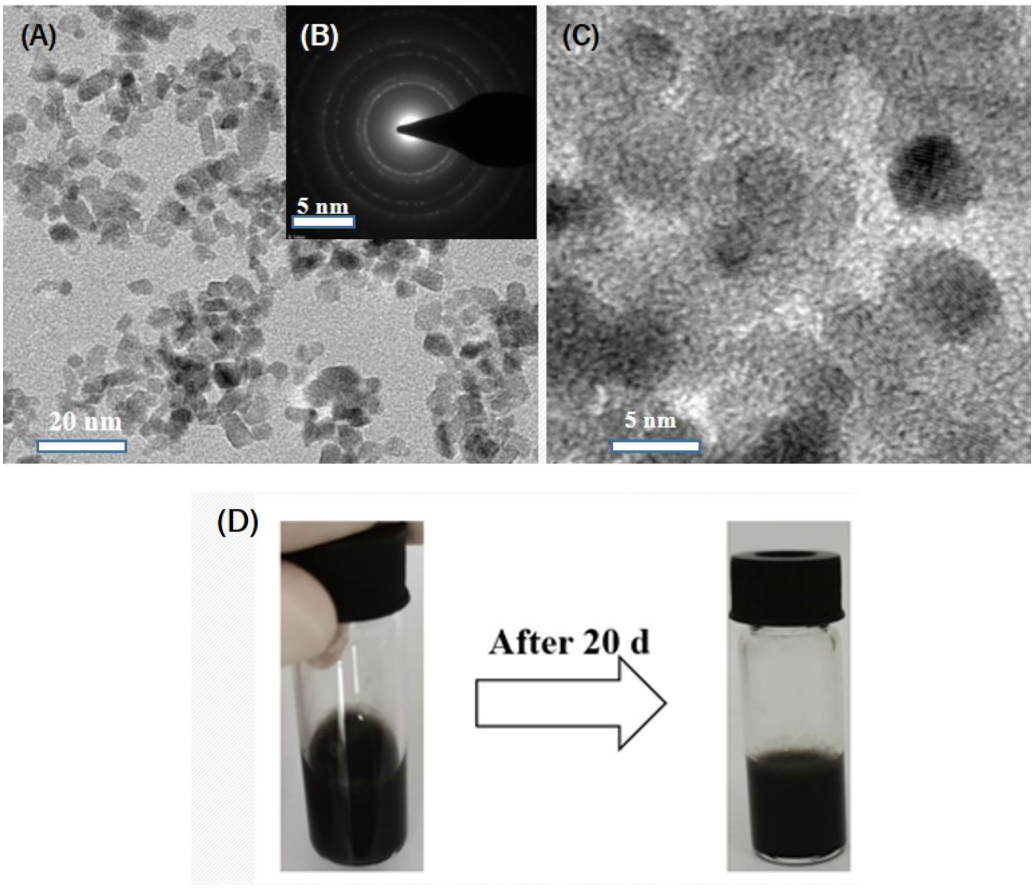

Figure S13. (A) TEM image of NiOx NPs, inset in (B) is corresponding SAED pattern. (C) HRTEM image of NiO_x NPs. (D) The photographs of NiO_x NPs was dispersed in water (30 mg/mL) stored in room temperature in air before and after 20 days.

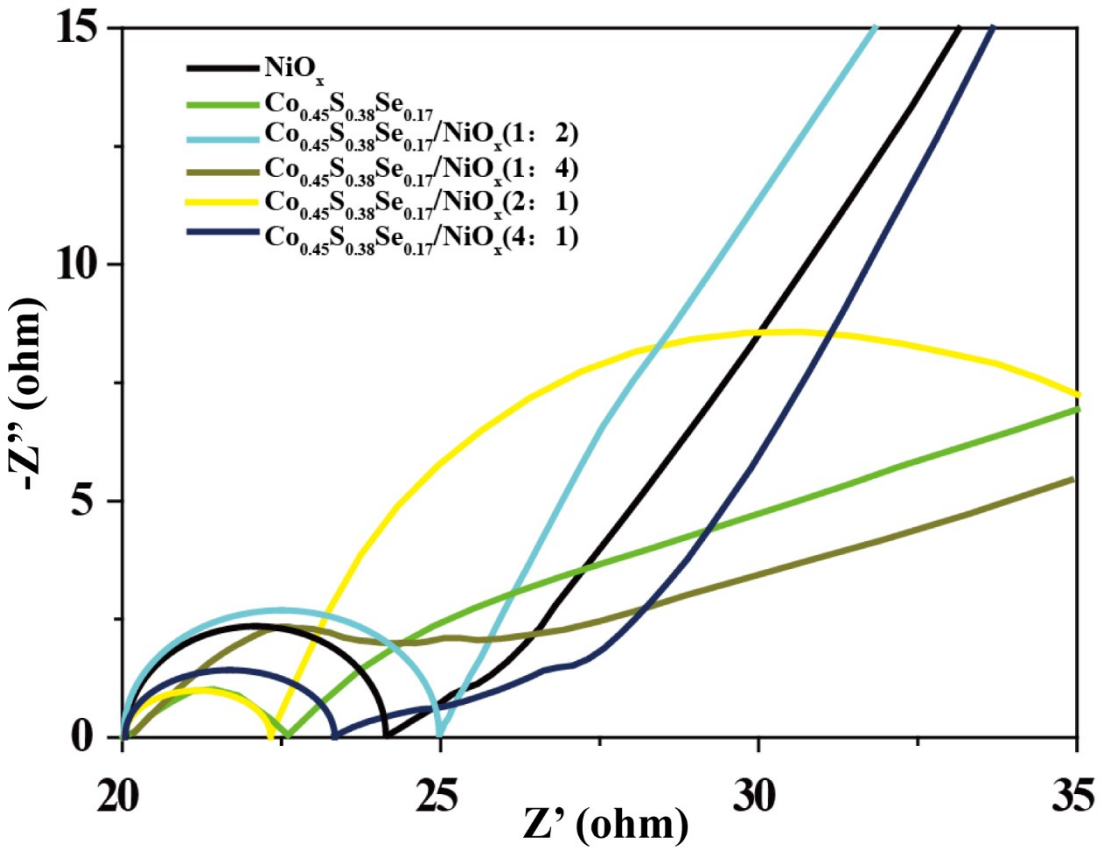

Figure S14. EIS plots for $Co_{0.45}S_{0.38}Se_{0.17}$ recombined with NiO_x at different ratios of 1:2, 1:4, 2:1, 4:1 respectively.

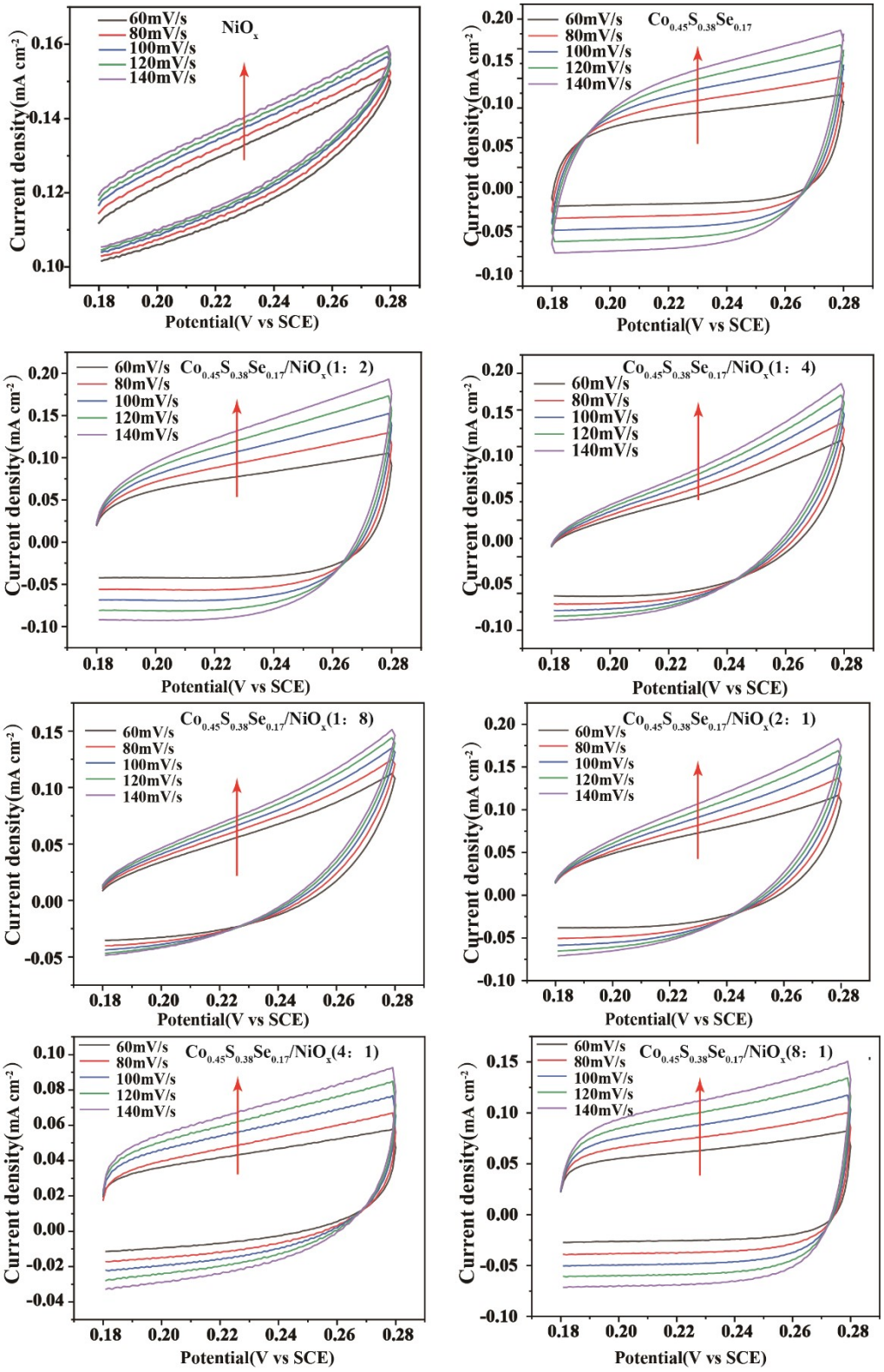

Figure S15. CV curves of $Co_{0.45}S_{0.38}Se_{0.17}$ recombined with NiO_x at different ratio of 1:2, 1:4, 1:8, 2:1, 4:1, 8:1 respectively, in the double layer at different scan rates.

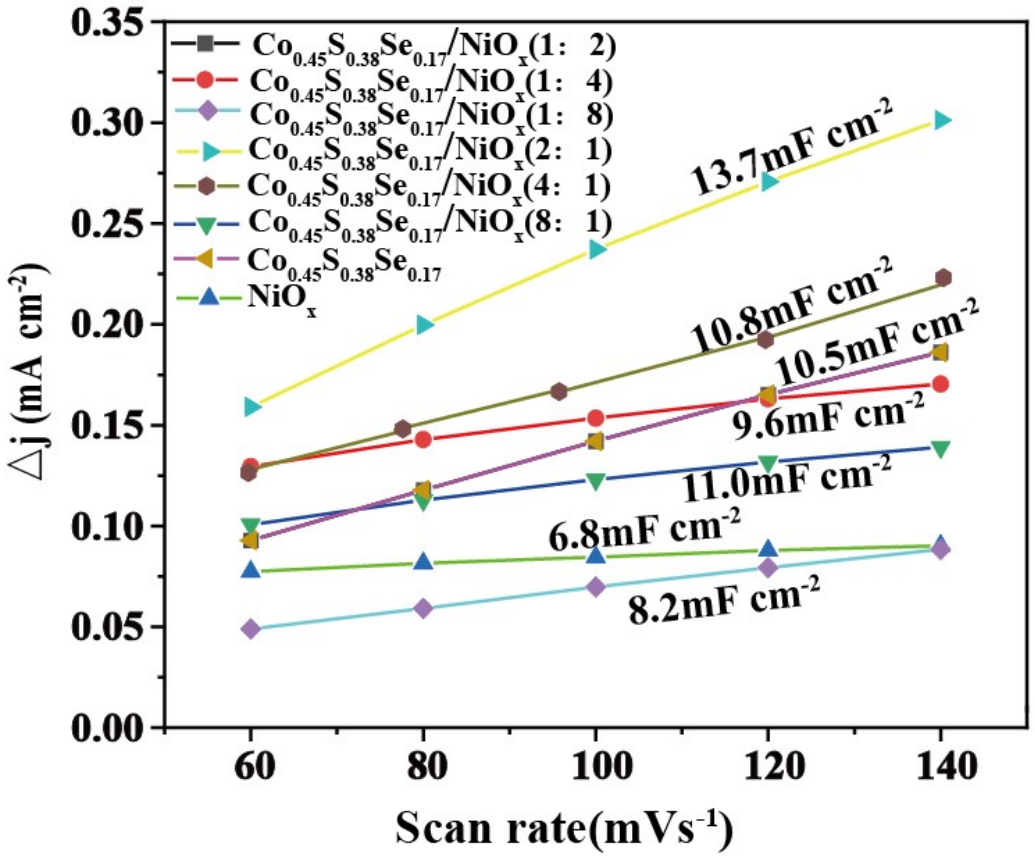

Figure S16. C*dl* of current density differences plotted against scan rates of $Co_{0.45}S_{0.38}Se_{0.17}$ recombined with NiO_x at different ratio of 1:2, 1:4, 1:8, 2:1, 4:1, 8:1, respectively.

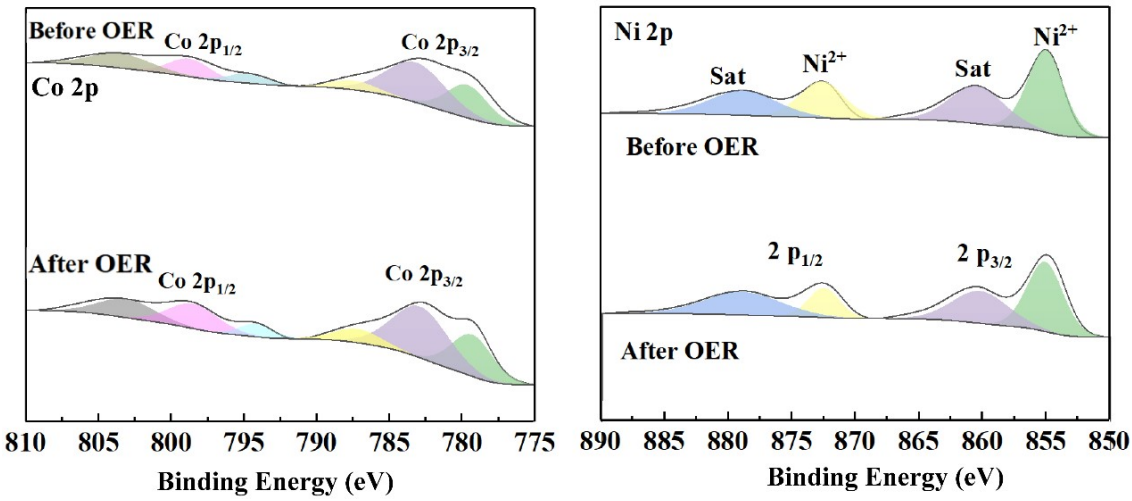

Figure S17. XPS spectra of $Co_{0.45}S_{0.38}Se_{0.17}/NiO_x$-2:1 before and after the stability test for OER.

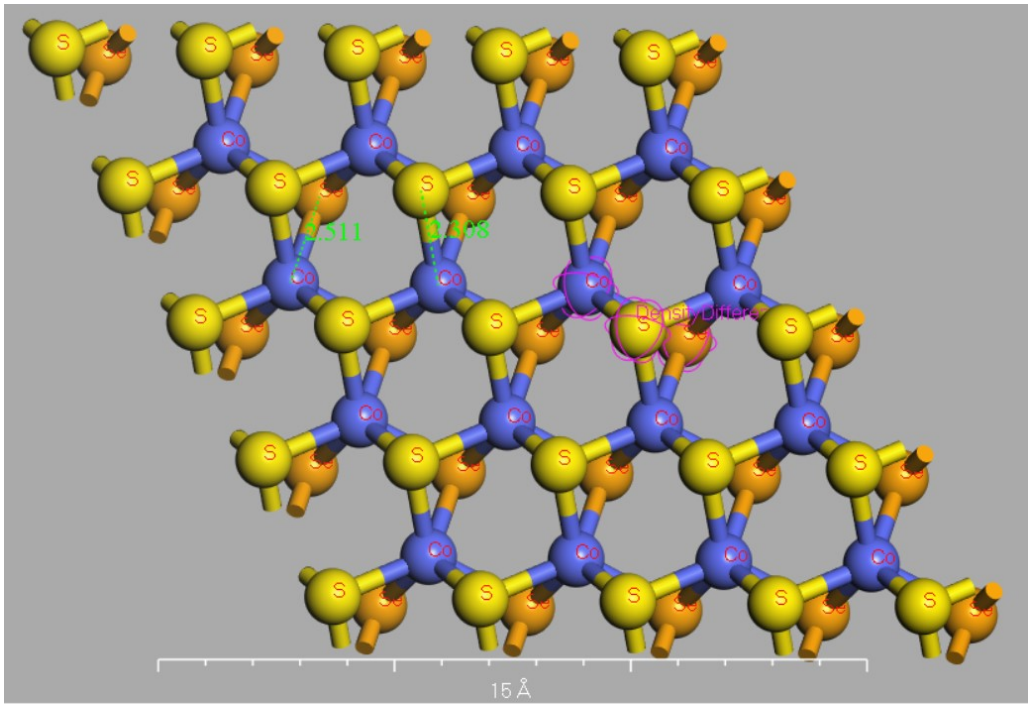

Figure S18. Optimized crystal structure for Co-S-Se monolayers and charge density for Co, S, Se atoms on the Co-S-Se monolayers. Bonds length are in Å.

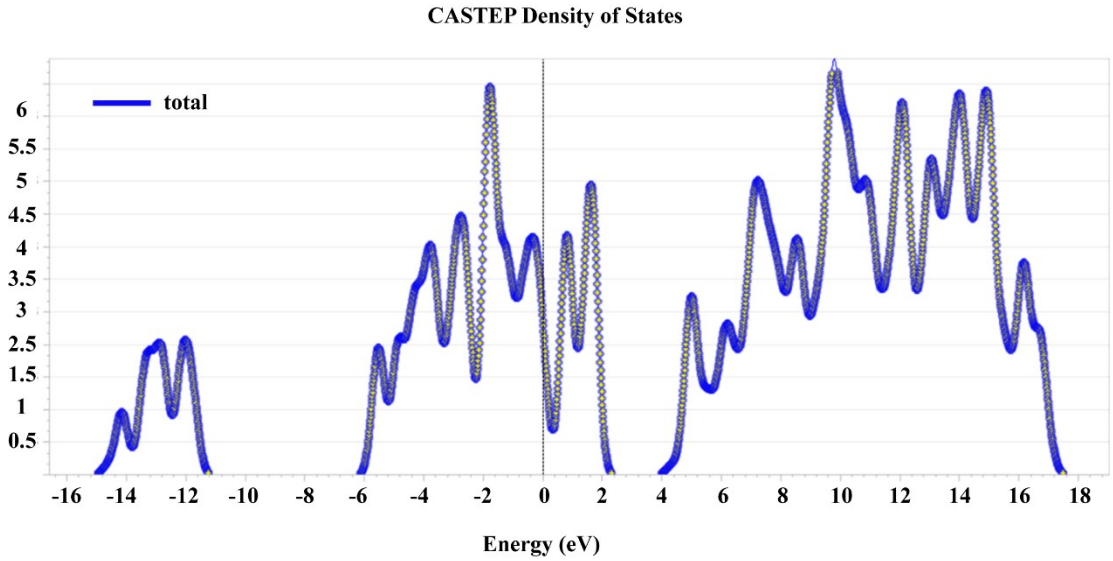

Figure S19. Density of states of Co-S-Se monolayers.

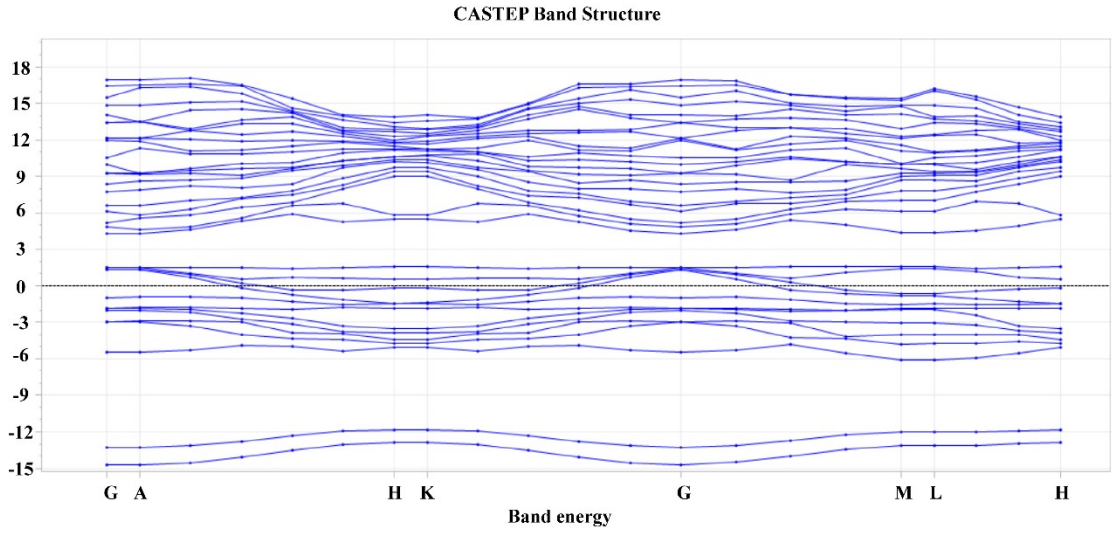

Figure S20. Band structure of Co-S-Se monolayers.

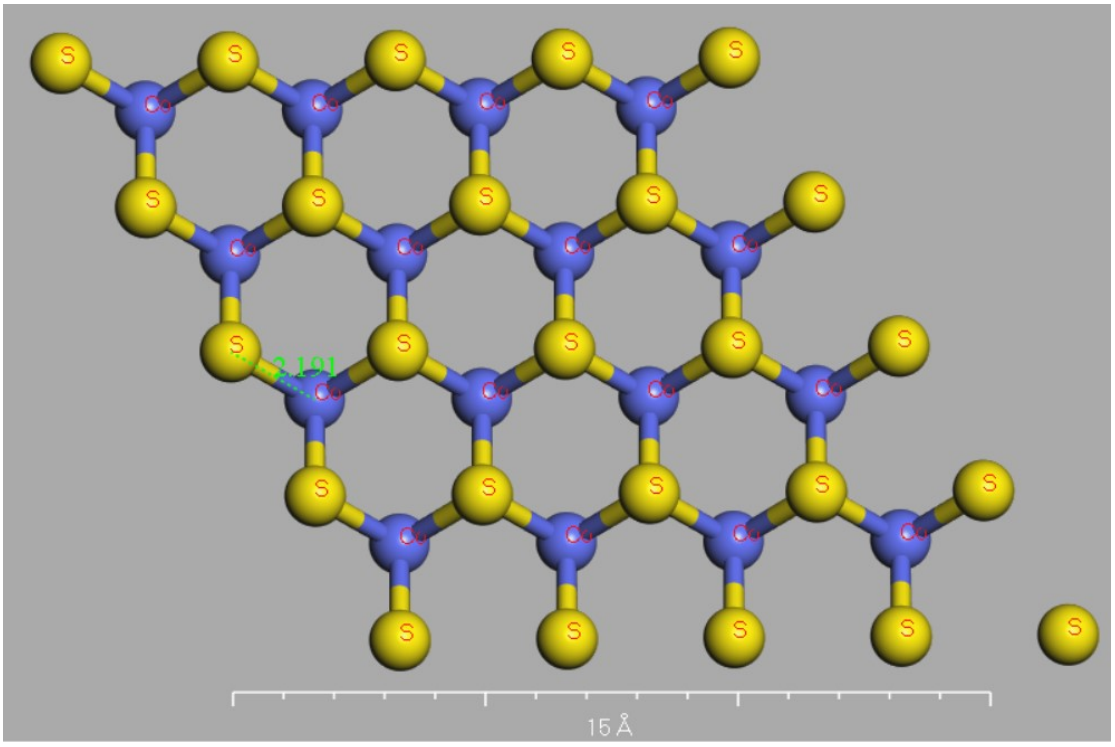

Figure S21. Optimized crystal structure for CoS_2 monolayers. Bonds length are in Å.

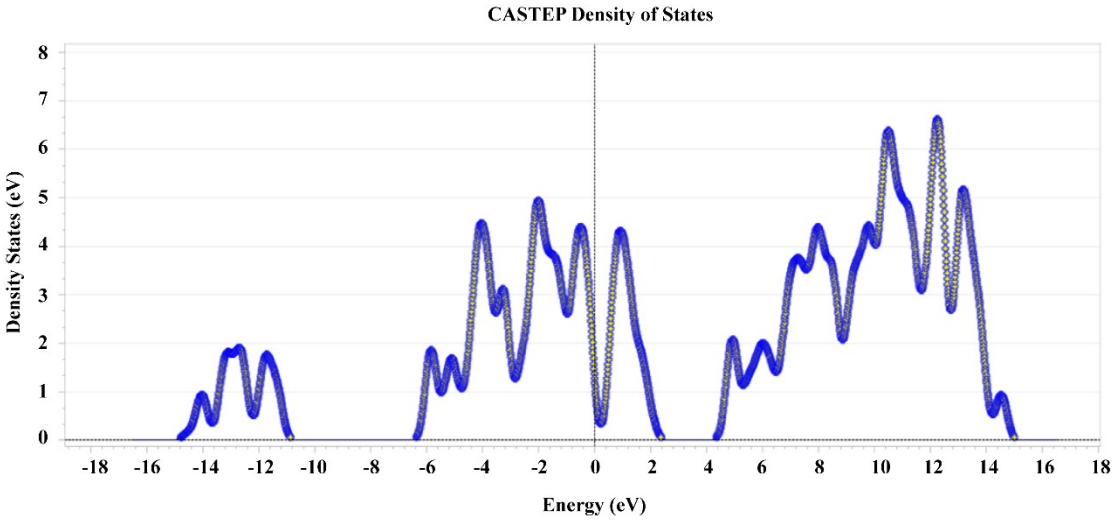

Figure S22. Density of states of CoS_2 monolayers.

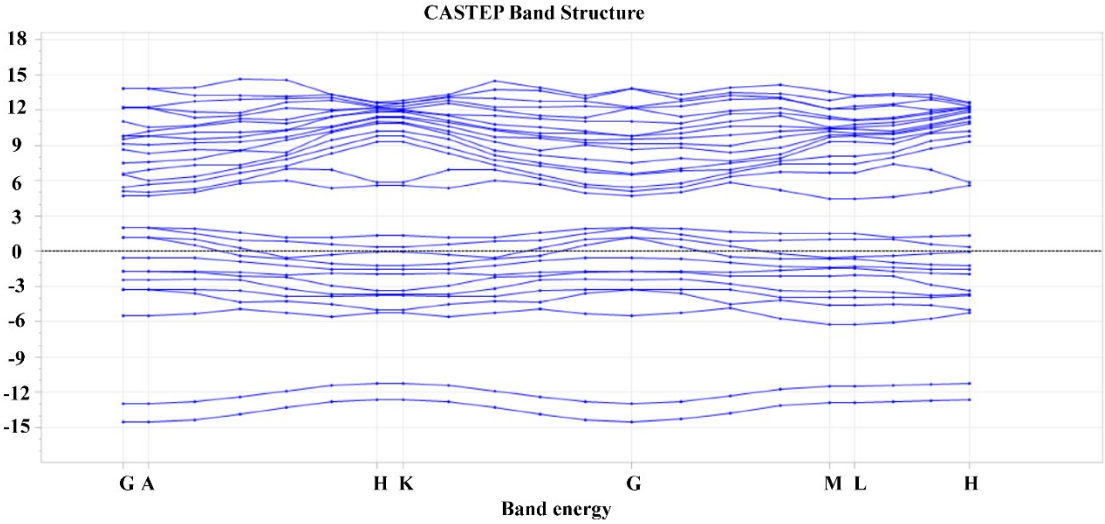

Figure S23. Band structure of CoS_2 monolayers.

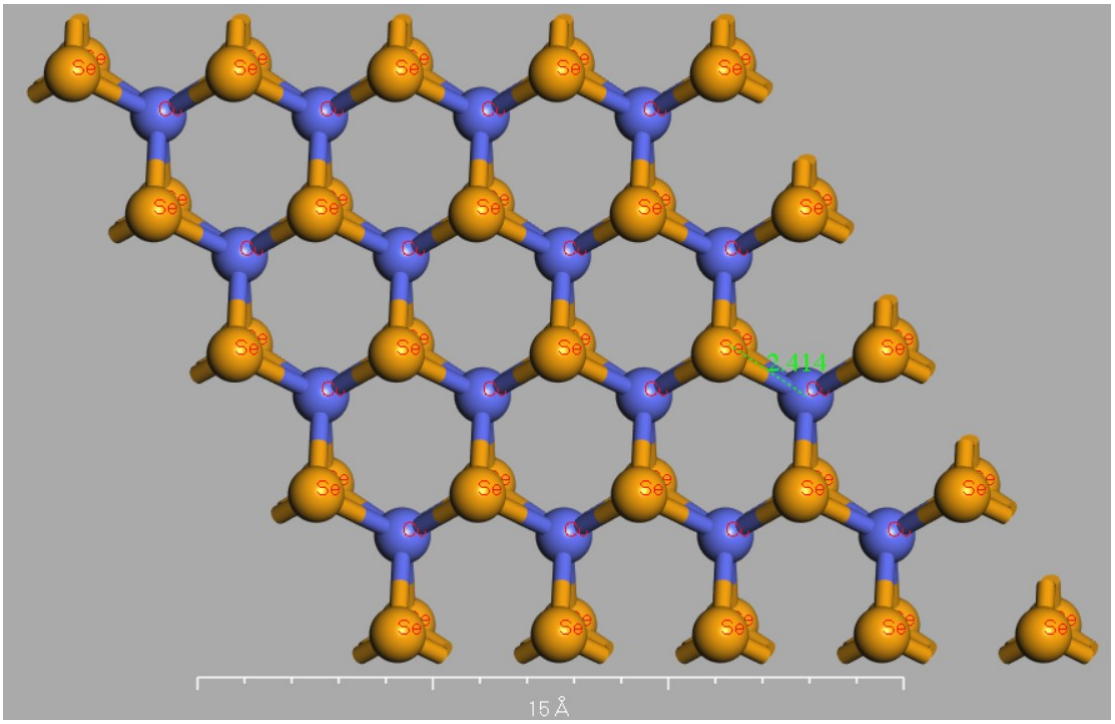

Figure S24. Optimized crystal structure for $CoSe_2$ monolayers. Bonds length are in Å.

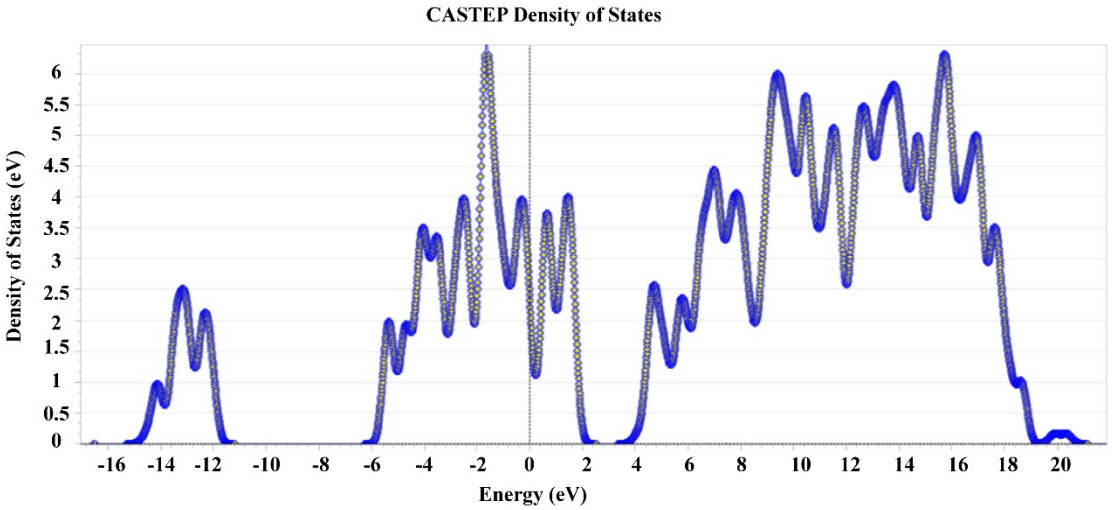

Figure S25. Density of states of $CoSe_2$ monolayers.

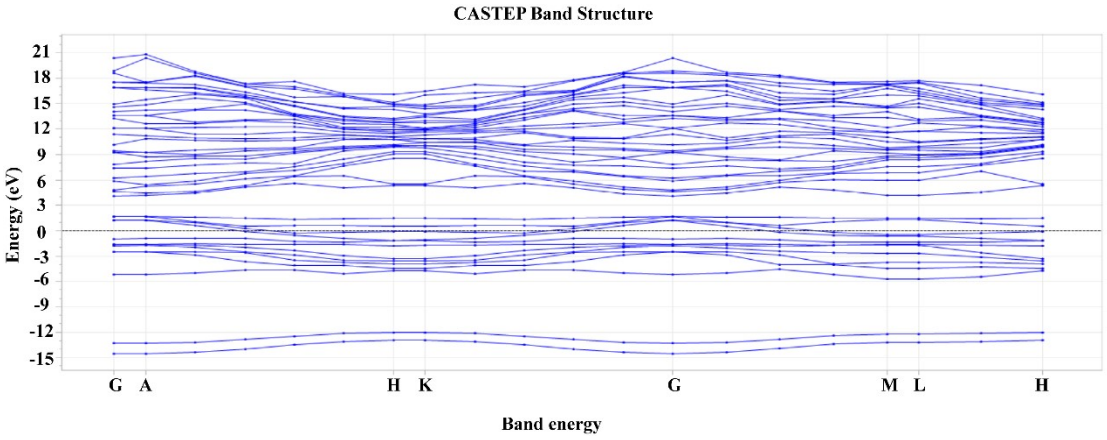

Figure S26. Band structure of $CoSe_2$ monolayers.

Reference

[1] Kresse, G.; Hafner, J. Ab initio molecular-dynamics simulation of the liquid metal amorphous semiconductor transition in germanium. *Physical Review B* **1994**, *49*, 14251.

[2] Perdew, J. P.; Burke, K.; Ernzerhof. M. Generalized Gradient Approximation Made Simple. *Physical Review Letters* **1996**, *77*, 3865.

[3] Mihailetchi, V. D.; Wildeman, J.; Blom. P. W. M. Space-Charge Limited Photocurrent. *Physical Review Letters* **2005**, *94*, 126602.